ChemComm

COMMUNICATION

View Article Online
View Journal | View Issue

Cite this: *Chem. Commun.*, 2016, **52**, 5049

Received 22nd December 2015,
Accepted 10th March 2016

DOI: 10.1039/c5cc10491b

www.rsc.org/chemcomm

A highly sensitive electrochemiluminescence biosensor for the detection of organophosphate pesticides based on cyclodextrin functionalized graphitic carbon nitride and enzyme inhibition†

Bingxin Wang, Haijun Wang, Xia Zhong,* Yaqin Chai, Shihong Chen and Ruo Yuan*

A signal on an electrochemiluminescence (ECL) biosensor using β-cyclodextrin (CD) functionalized graphitic carbon nitride (g-C_3N_4) as the luminophore was constructed for sensitive organophosphate pesticides (OPs) detection based on the enzyme inhibition of OPs, showing that the consumption of coreactant triethylamine (Et_3N) decreased with a lessening of the acetic acid (HAc) *in situ* generated by enzymatic reaction.

Organophosphates (OPs), acutely toxic substances, raise serious human health and environmental concerns due to the irreversible inhibition of acetylcholinesterase (AChE).[1–3] The conventional measurement techniques for OPs, such as gas or liquid chromatography and mass spectrometry, are accurate and reliable.[4–6] However, these methods need expensive instruments, complex operations, and trained personnel. Therefore, a simple, low-cost, and effective OP analysis technique is urgently needed. Electrochemiluminescence (ECL) is an attractive technique because of its simplified optical setup, low background noise and high sensitivity detection.[7–9]

As a new ECL luminophore, graphitic carbon nitride (g-C_3N_4) presents charming advantages because of its stable *s*-triazine ring structure and excellent photochemical properties compared with other ECL luminophores.[10,11] However, a conjugated, two-dimensional polymer of *s*-triazine tends to form a π-conjugated plane, and the stacking with optimized van der Waals interactions between the single layers of g-C_3N_4 make it deposit in most solvents.[12,13] Therefore, developing a better-performing method to improve the dispersity of g-C_3N_4 is of great interest.

β-Cyclodextrin (CD) is toroidal in shape with a hydrophobic inner cavity and a hydrophilic exterior containing lots of –OH groups.[14] These interesting characteristics can enable CD to selectively bind to various guest molecules.[15] Furthermore, the functional materials modified with CD could possess supramolecular recognition, good dispersion and high luminous efficiency.[16–18] Therefore, it is conceivable that using CD to functionalize g-C_3N_4 can successfully achieve the improvement of dispersity, amplification of the signal and recognition of the host–guest as a result.

Enzyme-based inhibition biosensors have emerged as a promising alternative to rapidly detect OPs, where AChE as an indicator could hydrolyze the acetylthiocholine (ATCl) into thiocholine and acetic acid (HAc).[19–21] In previous reports, most of OP detection methods were based on the amount change of thiocholine.[22,23] However, few research studies have been reported about using HAc as a quantitative entry point for OP detection. And as we know, the acid–base reaction has been widely applied due to its simple, fast and stable chemical properties. Therefore, making an acid–base reaction apply to OP determination based on HAc *in situ* generated *via* enzyme reaction would lead to efficient and sensitive detection.

Herein, CD as an enhancer was chemically decorated onto the surface of g-C_3N_4 to form a new nanocomposite of g-C_3N_4–CD. The host–guest inclusion complex (g-C_3N_4–CD–Fc-COOH) obtained *via* supramolecular recognition between ferrocenecarboxylic acid (Fc-COOH) and g-C_3N_4–CD could effectively immobilize AChE *via* an amidation reaction between the carboxyl group of Fc-COOH and the amino group of the enzyme. The resultant g-C_3N_4–CD–Fc-COOH/AChE was used to construct a signal on an ECL biosensor for OP detection *via* enzyme inhibition. When OPs were absent, AChE hydrolyzed the substrate acetylthiocholine (ATCl) to *in situ* generate acetic acid (HAc) which could react with triethylamine (Et_3N), a typical coreactant for the ECL of g-C_3N_4, around the electrode surface, resulting in an obviously decreased ECL signal. When OPs were present, OPs could inhibit the activity of AChE, and then the HAc yield decreased accompanied with lessening the consumption of coreactant Et_3N, inducing an enhanced

Key Laboratory of Luminescent and Real-Time Analytical Chemistry (Southwest University), Ministry of Education, College of Chemistry and Chemical Engineering, Southwest University, Chongqing 400715, P. R. China.
E-mail: zhonglyx@swu.edu.cn, yuanruo@swu.edu.cn; Fax: +86-23-68253172; Tel: +86-23-68252277

† Electronic supplementary information (ESI) available: Experimental section; characterizations of different nanocomposites; ECL and CV characterization of stepwise fabrication of the electrode; optimization of experimental conditions; stability and reproducibility. See DOI: 10.1039/c5cc10491b

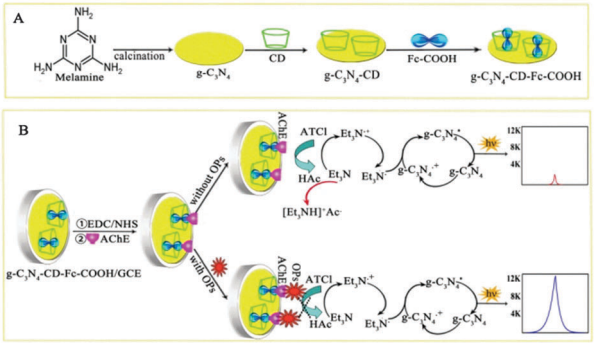

Scheme 1 (A) Preparation process of the g-C_3N_4–CD–Fe-COOH nanocomposite. (B) Schematic description of the fabrication of the proposed biosensor and the response mechanism.

ECL signal. The schematic diagram of the preparation process of the nanocomposite and the response mechanism is shown in Scheme 1.

The stability of g-C_3N_4–CD was supported by the fact that the g-C_3N_4–CD suspension (Fig. 1B) remained homogeneous for 10 days under ambient conditions, and was much more stable than the g-C_3N_4 suspension (Fig. 1A). In addition, the contact angle experiment was monitored on a glass slide with a water droplet of g-C_3N_4 and g-C_3N_4–CD. The contact angle for g-C_3N_4–CD was 44.1° (Fig. 1D), which was smaller than that for g-C_3N_4 (54.6°, Fig. 1C) due to the rich hydrophilic hydroxyl groups of CD. The results revealed that the incorporation of CD could improve the hydrophilic character of g-C_3N_4.

TEM was used to investigate the morphologies of the g-C_3N_4, g-C_3N_4–CD and g-C_3N_4–CD–Fe-COOH nanocomposites. g-C_3N_4 (Fig. 2A) showed the layers of a stack bulk structure, corresponding to the literature.[24] The black part of g-C_3N_4 indicated that the electron beam hardly penetrated through the layers because of the thick structure. In contrast, g-C_3N_4–CD (Fig. 2B) exhibited an ultrathin sheet structure with edge warping caused by the extreme lack of thickness, leading to a high surface-area-to-volume ratio. The reason might be as follows: firstly, the hydrophilic exterior of CD could improve the dispersity of g-C_3N_4 and lead to the stretch of the bulk structure; secondly, the CD molecule could prevent aggregation of g-C_3N_4. In Fig. 2C, g-C_3N_4–CD–Fe-COOH also presented a similar structure to g-C_3N_4–CD. Meanwhile, SEM also was applied in the morphology characterization of nanocomposites, which was in good agreement with the TEM observation. UV-vis and FT-IR (Fig. S1, ESI†) were used to further support the successful synthesis of the g-C_3N_4–CD–Fe-COOH nanocomposite.

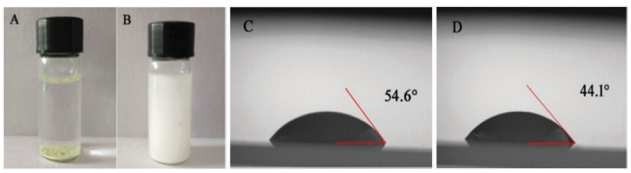

Fig. 1 Photographs of (A) g-C_3N_4 and (B) g-C_3N_4–CD dispersed in water stand for 10 days. The shape of a water droplet on the glass slide of (C) g-C_3N_4 and (D) g-C_3N_4–CD.

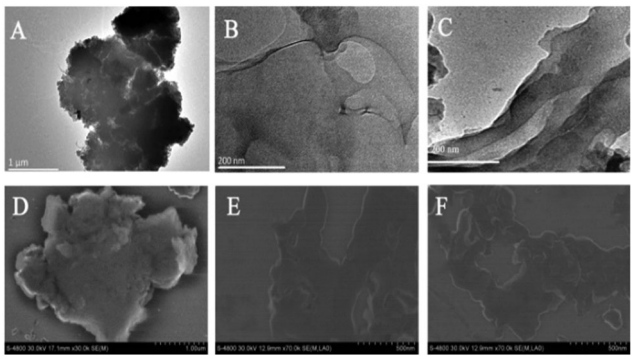

Fig. 2 TEM image of (A) g-C_3N_4, (B) g-C_3N_4–CD, and (C) g-C_3N_4–CD–Fe-COOH. SEM image of (D) g-C_3N_4, (E) g-C_3N_4–CD, and (F) g-C_3N_4–CD–Fe-COOH.

In order to investigate the ECL signal of g-C_3N_4–CD–Fe-COOH, different modified electrodes were prepared, including g-C_3N_4/GCE, g-C_3N_4–CD/GCE and g-C_3N_4–CD–Fe-COOH/GCE. As shown in Fig. 3A, the ECL signal of g-C_3N_4/GCE was observed obviously (curve a). The luminous mechanism of g-C_3N_4 was concluded as follows:[25]

$$\text{g-}C_3N_4\text{–e} \rightarrow \text{g-}C_3N_4^{\bullet+} \quad (1)$$

$$Et_3N\text{–e} \rightarrow Et_3N^{\bullet+} \quad (2)$$

$$Et_3N^{\bullet+}\text{–}H^+ \rightarrow Et_3N^{\bullet} \quad (3)$$

$$\text{g-}C_3N_4^{\bullet+} + Et_3N^{\bullet} \rightarrow \text{g-}C_3N_4^{*} + Et_3N_{ox} \quad (4)$$

$$\text{g-}C_3N_4^{*} \rightarrow \text{g-}C_3N_4 + h\nu \quad (5)$$

As shown in eqn (1), when the applied potential is more positive than the valence band of g-C_3N_4, g-C_3N_4 might be electro-oxidized to form the positively charged g-C_3N_4 (*i.e.*, g-$C_3N_4^{\bullet+}$). The cation ($Et_3N^{\bullet+}$) could be produced from the electro-oxidation of coreactant Et_3N (eqn (2)), which released a proton to form a radical ($Et_3N^{\bullet}$), as shown in eqn (3). The electro-oxidized semiconductors g-$C_3N_4^{\bullet+}$ could react with radical $Et_3N^{\bullet}$ to generate the excited state g-$C_3N_4^{*}$ *via* electron transfer (eqn (4)). The excited state g-$C_3N_4^{*}$ decayed back to the ground state g-C_3N_4, leading to an intense emission (eqn (5)). When CD functionalized g-C_3N_4 was modified on GCE, the ECL response of g-C_3N_4–CD/GCE

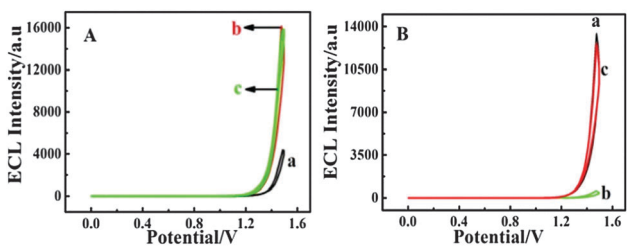

Fig. 3 (A) ECL response of (a) g-C_3N_4/GCE, (b) g-C_3N_4–CD/GCE, and (c) g-C_3N_4–CD–Fe-COOH/GCE in 0.1 M PBS containing 50 mM Et_3N. (B) ECL response of AChE/g-C_3N_4–CD–Fe-COOH/GCE (a) without 100 μM ATCl and 0.5 μM OPs, (b) with 100 μM ATCl and (c) with both 100 μM ATCl and 0.5 μM OPs.

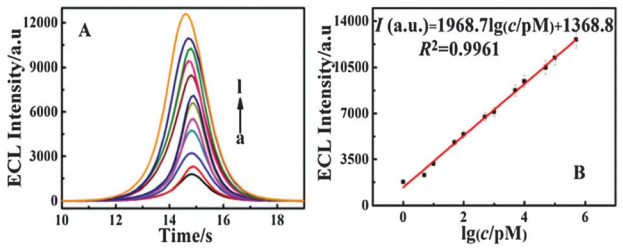

Fig. 4 (A) ECL response of the biosensor to ethyl paraoxon with the concentration: (a) 1×10^{-12}, (b) 5×10^{-12}, (c) 1×10^{-11}, (d) 5×10^{-11}, (e) 1×10^{-10}, (f) 5×10^{-10}, (g) 1×10^{-9}, (h) 5×10^{-9}, (i) 1×10^{-8}, (j) 5×10^{-8}, (k) 1×10^{-7}, and (l) 5×10^{-7} M. (B) The calibration curve for ethyl paraoxon.

(curve b) was four times higher than that of g-C_3N_4/GCE. The reason might be as follows. Firstly, CD possesses rich hydroxyl groups which as electron-donating groups tend to increase the ECL intensity.[26] Secondly, when the hydroxy and amine groups were coexistent, the ECL response is much higher because the hydroxy group could catalyze the oxidation of amines.[27] The ECL response of g-C_3N_4–CD–Fc-COOH/GCE (curve c) was slightly less than curve b, which may be attributed to the existence of Fe(III). The results revealed that the incorporation of CD improved the luminous efficiency of g-C_3N_4.

In order to confirm the fabrication process of the modified electrode, ECL and CV characterizations were investigated. The results are exhibited in Fig. S2 (ESI†).

The mechanism of OP detection was studied in detail based on enzyme inhibition in PBS (0.1 M, pH 7.0) with 50 mM Et_3N. As seen in Fig. 3B, the ECL response of AChE/g-C_3N_4–CD–Fc-COOH/GCE was strong (curve a). When 0.1 mM ATCl was dropped into the detecting cell, the ECL response decreased obviously (curve b). The reason might be that AChE can catalyze the hydrolyzation of ATCl to *in situ* generate HAc which could react with the coreactant Et_3N around the electrode surface, resulting in an obvious decrease of the ECL signal. However, when OPs were present, the ECL signal increased obviously (curve c) because OPs could inhibit the enzyme activity and then reduce the consumption of Et_3N.

Under the optimum detection conditions (Fig. S3, ESI†), the performance of the proposed biosensor was evaluated by incubating the standard OP solution with different concentrations. As depicted in Fig. 4, the ECL intensity gradually increased with the concentration of OPs increasing. The reason might be that OPs inhibited the enzyme activity and induced a low yield of HAc. The consumption of Et_3N decreased with the yield of HAc decreasing, leading to a signal on ECL. The corresponding linear equation was I (a.u.) = 1968.7 lg(c/pM) + 1368.8 (where I was the ECL intensity and c was the concentration of OPs), with a correlation coefficient R^2 = 0.996. Compared with other biosensors for OPs detection (Table S1, ESI†[28–31]), the proposed biosensor exhibited a lower detection limit of 0.3 pM (S/N = 3), and the linear range was from 1.0 pM to 0.5 μM, achieving six orders of magnitude, which might hold a new promise for the highly sensitive and ultratrace detection of OPs. In addition, the excellent stability and reproducibility of the biosensor are exhibited in Fig. S4 (ESI†).

To further evaluate the practicality of the proposed electrode in the detection of real-life samples, the recovery experiment was performed in the supernatant of different vegetable samples using a standard addition method. The recoveries are presented in Table S2 (ESI†) from 94.2% to 108.4%. The results demonstrated that the ECL biosensor had a potential application to analyze practical samples.

In conclusion, a novel signal on an ECL biosensor was applied for OP detection based on CD functionalized g-C_3N_4 and the enzyme inhibition reaction. Compared with pure g-C_3N_4, g-C_3N_4 modified with CD possessed good dispersity, stability, supramolecular recognition and luminous efficiency. Since HAc *in situ* generated *via* an enzymatic reaction could rapidly consume coreactant Et_3N, the biosensor based on the proposed enzyme inhibition reaction exhibited the advantage of high sensitivity, low background signal and rapid response. Therefore, such a new ECL biosensor opened up a new direction for fast and immediate OP detection in various samples.

This work was financially supported by the NNSF of China (21275119, 21575116, 51473136), Natural Science Foundation of Chongqing City (CSTC-2014JCYJA20005), the Doctor Foundation of Southwest University (swu113029) and the Fundamental Research Funds for the Central Universities (XDJK2013C115, XDJK2015A002), China.

Notes and references

1 X. J. Du, D. Jiang, N. Hao, Q. Liu, J. Qian, L. M. Dai, H. P. Mao and K. Wang, *Chem. Commun.*, 2015, **51**, 11236–11239.
2 G. Aragay, F. Pino and A. Merkoci, *Chem. Rev.*, 2012, **112**, 5317–5338.
3 M. Ali, S. Nasir, I. Ahmed, L. Fruk and W. Ensinger, *Chem. Commun.*, 2013, **49**, 8770.
4 J. Lee and H. K. Lee, *Anal. Chem.*, 2011, **83**, 6856–6861.
5 P. Payá, M. Anastassiades, D. Mack, I. Sigalova, B. Tasdelen, J. Oliva and A. Barba, *Anal. Bioanal. Chem.*, 2007, **389**, 1697–1714.
6 T. Zhou, X. H. Xiao and G. K. Li, *Anal. Chem.*, 2012, **84**, 5816–5822.
7 X. Y. Jiang, Y. Q. Chai, H. J. Wang and R. Yuan, *Biosens. Bioelectron.*, 2014, **54**, 20–26.
8 L. Dennany, R. J. Forster and J. F. Rusling, *J. Am. Chem. Soc.*, 2003, **125**, 5213–5218.
9 L. L. Liu, Q. Ma, L. Yang, Z. P. Liu and X. G. Su, *Biosens. Bioelectron.*, 2015, **63**, 519–524.
10 L. C. Chen, X. T. Zeng, P. Si, Y. M. Chen, Y. W. Chi, D. H. Kim and G. N. Chen, *Anal. Chem.*, 2014, **86**, 4188–4195.
11 X. Ou, X. R. Tan, X. F. Liu, Q. Y. Lu, S. H. Chen and S. P. Wei, *Biosens. Bioelectron.*, 2015, **70**, 89–97.
12 X. C. Wang, S. Blechert and M. Antonietti, *ACS Catal.*, 2012, **2**, 1596–1606.
13 Y. Wang, X. C. Wang and M. Antonietti, *Angew. Chem., Int. Ed.*, 2012, **51**, 68–89.
14 A. Douhal, *Chem. Rev.*, 2004, **104**, 1955–1976.
15 K. Shang, X. D. Wang, B. Sun, Z. Q. Cheng and S. Y. Ai, *Biosens. Bioelectron.*, 2013, **45**, 40–45.
16 H. Dai, C. P. Yang, X. L. Ma, Y. Y. Lin and G. N. Chen, *Chem. Commun.*, 2011, **47**, 11915–11917.
17 Q. Chen, H. Chen, Y. Y. Zhao, F. Zhang, F. Yang, J. Tang and P. G. He, *Biosens. Bioelectron.*, 2014, **54**, 547–552.
18 Y. J. Guo, S. J. Guo, J. T. Ren, Y. M. Zhai, S. J. Dong and E. K. Wang, *ACS Nano*, 2010, **4**, 4001–4010.
19 C. Zhai, X. Sun, W. P. Zhao, Z. L. Gong and X. Y. Wang, *Biosens. Bioelectron.*, 2013, **42**, 124–130.
20 L. H. Hess, A. Lyuleeva, B. M. Blaschke, M. Sachsenhauser, M. Seifert, J. A. Garrido and F. Deubel, *ACS Appl. Mater. Interfaces*, 2014, **6**, 9705–9710.
21 D. S. Guo, V. D. Uzunova, X. Su, Y. Liu and W. M. Nau, *Chem. Sci.*, 2011, **2**, 1722–1734.
22 H. Liang, D. D. Song and J. M. Gong, *Biosens. Bioelectron.*, 2014, **53**, 363–369.
23 L. Zhang, A. D. Zhang, D. Du and Y. H. Lin, *Nanoscale*, 2012, **4**, 4674–4679.

24 J. Q. Tian, Q. Liu, C. J. Ge, Z. C. Xing, A. M. Asiri, A. O. Al-Youbicd and X. P. Sun, *Nanoscale*, 2013, **5**, 8921–8924.
25 Y. T. Liu, Q. B. Wang, J. P. Lei, Q. Hao, W. Wang and H. X. Ju, *Talanta*, 2014, **122**, 130–134.
26 X. Q. Liu, L. H. Shi, W. X. Niu, H. J. Li and G. B. Xu, *Angew. Chem., Int. Ed.*, 2007, **46**, 421–424.
27 L. H. Zhang, X. Q. Zou, E. B. Ying and S. J. Dong, *J. Phys. Chem. C*, 2008, **112**, 4451–4454.
28 R. K. Mishra, R. B. Dominguez, S. Bhand, R. Munoz and J. Marty, *Biosens. Bioelectron.*, 2012, **32**, 56–61.
29 Y. Q. Yang, H. Y. Tu, A. D. Zhang, D. Du and Y. H. Lin, *J. Mater. Chem.*, 2012, **22**, 4977–4981.
30 Y. Q. Yang, A. M. Asiri, D. Du and Y. H. Lin, *Analyst*, 2014, **139**, 3055–3060.
31 Y. Ivanov, I. Marinov, M. Portaccio, M. Lepore, D. G. Mita and T. Godjevargova, *Biotechnol. Biotechnol. Equip.*, 2012, **26**, 3044–3053.

